Novel gold nanoparticles coated with somatostatin as a potential delivery system for targeting somatostatin receptors

Journal:	*Drug Development and Industrial Pharmacy*
Manuscript ID	LDDI-2015-0563
Manuscript Type:	Original Research Paper
Date Submitted by the Author:	02-Oct-2015
Complete List of Authors:	Abdellatif, Ahmed A.H.; Pharmaceutics and Industrial Pharmacy, Faculty of Pharmacy, Al-Azhar University, Assuit, Egypt, Zayed, Gamal; Pharmaceutics and Industrial Pharmacy, Faculty of Pharmacy, Al-Azhar University, Assuit, Egypt, Saleem, Imran; School of Pharmacy and Chemistry, Liverpool John Moores University, Liverpool, UK, Tawfeek, Hesham; Industrial Pharmacy Department, Faculty of Pharmacy, Assiut University, Assiut, Egypt,
Keywords:	Somatostatin acetate, citrate gold nanoparticles, HCC-1806 cell lines, nanoparticles targeting, somatostatin targeting

Novel gold nanoparticles coated with somatostatin as a potential delivery system for targeting somatostatin receptors

Ahmed A. H. Abdellatif[1], *Gamal Zayed*[1], *Imran Y. Saleem*[3] *and Hesham M. Tawfeek*[2]

[1]Faculty of Pharmacy, Department of Pharmaceutics and Industrial Pharmacy, Al-Azhar University, Assiut, Egypt.

[2]Faculty of Pharmacy, Department of Industrial Pharmacy, Assiut University, Assiut, Egypt.

[3]School of Pharmacy and Biomolecular Science, Liverpool John Moores University, Liverpool, UK.

Corresponding author:

Dr: Hesham Mohamed Tawfeek

Lecturer of Industrial Pharmacy
Address: Faculty of Pharmacy, Department of Industrial Pharmacy, Assiut University, Assiut, Egypt.
Email Address: Hesham.hassan@pharm.au.edu.eg
Phone: +2010 265 17179

Key words:

Somatostatin acetate, citrate gold nanoparticles, HCC-1806 cell lines, nanoparticles targeting, somatostatin targeting.

Abstract

Targeting of G-protein coupled receptors (GPCRs) like somatostatin (SST) could have a potential interest in delivery of anti-cancer agents to tumor cells. Attachment of SST to different nano-carriers e.g., polymeric nanoparticles is limited due to the difficulty of interaction between SST itself and those nano-carriers. Furthermore, the instability problems associated with the final formulation. Attaching of SST to gold nanoparticles (AuNPs) using the positive and negative charge of SST and citrate-AuNPs could be considered a new technique to get stable non-aggregated AuNPs coated with SST. Different analyses techniques have been performed to proof the principle of coating between AuNPs and SST. Furthermore, cellular uptake study on HCC-1809 cell lines has been investigated to show the ability of AuNPs coated SST to enter the cells via SST receptors. Dynamic light scattering (DLS) indicated a successful coating of SST on the MUA-AuNPs surface. Furthermore, all the performed analysis including DLS, SDS-PAGE and UV-VIS absorption spectra indicated a successful coating of AuNPs with SST. Cellular uptake study on HCC-1806 cell lines showed that the number of AuNPs-SST per cell is significantly higher compared to citrate-AuNPs when quantified using inductively coupled plasma spectroscopy. Moreover, the binding of AuNPs-SST to cells can be suppressed by addition of antagonist, indicating that the binding of AuNPs-SST to cells is due to receptor-specific binding. In conclusion, AuNPs could be attached to SST via adsorption to get stable AuNPs coated SST. This new formulation has a potential to target SST receptors localized in many normal and tumor cells.

Introduction

Gold nanoparticles (AuNPs) are considered to be very important and applicable tool in nanotechnology. This is due to their easy surface functionalization and/ or bio-conjugation, stability and biocompatibility. They have been the subjects of many studies and many applications in medicine and in biology, such as immunoassays, drug targeting of cancer cells and in biomedical research (1-2). AuNPs were delivered to ovarian cancer cells that express the epidermal growth factor receptor and the folate receptor, the ovarian cell took all particles by active transport (3). It was found that tumor cells can be killed by excitation of internalized AuNPs, the internalized AuNPs were excited by laser beam which killed the cancer cells (4).

SSTRs are members of the G-protein coupled receptors (GPCRs) super family (5-6). There are five different subtypes of SSTRs (SSTR1-5), $SSTR_2$ having been classified into two subtypes, $SSTR_{2A}$ and $SSTR_{2B}$ (7-8). The blocking of SSTRs with antagonist suppresses the interaction of the peptide agonist with SSTRs (9). SSTRs are present in the surface of numerous normal and diseased cells; they are expressed in normal tissues such as the pituitary gland and pancreas (8, 10). SSTRs are also expressed in many tumor cells i.e. small cell and non-small lung cancer lung cancer (11-13), neuroendocrine tumors and breast cancer (14).

Receptor-mediated endocytosis is an important example of a specific internalization mechanism following ligand binding to their receptor (15-17). It allows for an import of extracellular molecules for around 1000-fold increase of the intracellular concentration of macromolecules (18-20). In the process of endocytosis, the plasma membrane is engulfed inwards from specialized membrane micro-domains forming either clathrin or caveolin-coated pits (20).

SST has many functions in mammals, it can controls the secretion of growth hormones (21). Moreover, it is widely distributed throughout the central nervous system and peripheral tissues employing numerous roles in the central nervous system (22-23). Furthermore, SST inhibits the regulation of many endogenous cell functions, including the modulation of neurotransmission, motility, cell proliferation and cell secretion (24-25). Hence, SST could be considered promising molecules in drug delivery applications. The limited stability and the presence of many functional groups within SST make the interaction with other compounds such as PEGylation with thiolated-PEG is difficult. Many trials have been performed in our laboratory for PEGylation of SST or even attaching any other polymer to coat AuNPs. Such trials showed the difficulty of such attachment due to the numerous functional groups of SST. Moreover, it may affect the structure and integrity of SST.

Up to date and according to our research in literature we have the first attempt to rationally develop and formulate a novel stable non-aggregated AuNPs coated with SST. AuNPs coated with SST system has a potential to active target SST receptors for diagnostic as well as therapeutic purposes. The novel prepared system utilizing the absorption between the positively charged SST and the negatively charged citrate-AuNPs at neutral pH. AuNPs were prepared by citrate reduction method and coated with 11-MUA to facilitate the binding with SST. Furthermore, the stability and the ability to adsorb SST to either citrate-coated-AuNPs or 11-MUA-coated AuNPs were investigated. The prepared citrate-AuNPs, MUA-AuNPs and AuNPs coated with different concentrations of SST were examined for their size, polydispersity and surface charge. Moreover, the dissociation and adsorption of SST to AuNPs were also studied and confirmed using sodium dodecyl sulphate and

polyacrylamide gel electrophoresis. Cellular uptake study for citrate-AuNPs, AuNPs-SST and AuNPs-SST together with antagonist was also performed using HCC-1806 cell lines. In addition, the amounts of Au internalized into the cells were quantified using inductively coupled plasma spectroscopy (ICP-OES).

Materials and methods

Materials

Somatostatin acetate (SST) was kindly supplied from CuraMED Pharma GmbH (karlsruhe, Germany). Hydrogen tetrachloroaurate tri-hydrate, 11-Mercaptoundecanoic acid (11-MUA), RPMI 1640 medium, bovine serum albumen, Chloroauric acid ($HAuCl_4$) and cyn-154806 trifluoroacetate (TFA) were purchased from Sigma Aldrich (Steinheim, Germany). Tri-sodium citrate dihydrate, sodium chloride, sodium hydroxide, nitric acid, hydrochloric acid, triethylamine, sodium dihydrogen phosphate, disodium hydrogen phosphate were purchased from Merck (Darmstadt, Germany). Dulbecco`s phosphate buffered saline (pH 7.4), Dulbecco's Modified Eagle Medium, and Leibovitzs L-15 were purchased from Invitrogen, (Paisley, UK). Triple negative breast cancers cells (HCC-1806) were kindly supplied from Dr. Abdellatif Bouazzaoui (Haematology and Internal Oncology, Regensburg University, Germany). The purified water used for all experiment was obtained using a Milli-Q water purification system from Millipore (Schwalbach, Garmany). Any other chemicals and solvents were of analytical grade.

Preparation of AuNPs capped with SST

Preparation of citrate-AuNPs

First, citrate-AuNPs were prepared according to apreviously reported procedure (26-28). Briefly, 3mL of 38.8mM tri-sodium citrate solution were added to 100mL of 0.3mM Chloroauric acid ($HAuCl_4$) solution in a 250mL round bottom flask. The reaction mixture stirred vigorously and heated under reflux. Refluxing was continued for 15 minutes, and then the prepared AuNPs was left to cool at room temperature (28). Stirring was continued for an additional 15 minutes. AuNPs were purified from larger

aggregates by centrifugation for 30 minutes at 2,450 ×*g* using (Avanti centrifuge J-E/ Beckman coulter GmbH, Germany).

Stabilization of the synthesized citrate-AuNPs

11-MUA was deposited on the gold surface to facilitate the electrostatic binding between SST and AuNPs (29-31). Briefly, 1mL of 1mM stock solution of 11-MUA was added to 20mL of the prepared AuNPs solution in a 100mL Erlenmeyer flask. After adjusting the pH to 11, the AuNPs were incubated with 11-MUA under continuous stirring at 600rpm at room temperature overnight. This allows sufficient exchange of citrate anions with 11-MUA on the particle surface. The stabilized particles were purified by centrifugation at 15,700×*g* for 20 minutes in a falcon tube using an Avanti centrifuge J-E/ Beckman coulter GmbH, Germany. The supernatant was decanted and the precipitate was resuspended again in Millipore water (30).

Coating of MUA-AuNPs with SST

First, different concentrations of SST (20, 40, 60, 100 and 200nM) were studied to show the optimal concentration for coating. In brief, 3mL of the prepared MUA-AuNPs were mixed with 100µL of 10mM NaCl as isotonic solution and stirred for 30 minutes(32). Then the stabilized MUA-AuNPs were added drop-wise to 10µL of different concentrations of SST to determine the optimum concentration of SST that can load to AuNPs. The solution was stirred for another 30 minutes. The stabilized AuNPs-SST were purified by centrifugation at 15,700×g for 15 minutes, using (Eppendorf centrifuge 5415R, Hamburg, Germany), the supernatant was decanted and the precipitate was re-suspended again in Millipore water. The steps of deposition and purifications are shown in (Figure 1).

Insert Figure 1 here

Characterization of AuNPs capped with SST

Size and surface charge

To determine the size, count rate and zeta potential of AuNPs, the samples were adjusted to 25±1.0°C and laser light scattering analysis was performed with an incident laser beam of 633nm at a scattering angle of 90° using the Malvern zetasizer nano 6.01 (Malvern Instruments GmbH, Herrenberg, Germany). The sampling time was set automatically. Moreover, three measurements were allowed to perform each 10 sub-runs and, all measurements were carried out in aqueous solution. The results were calculated from the average of three independent measurements (28).

Dissociation of SST from AuNPs-SST by solid sodium dodecyl sulfate

Sodium dodecyl sulfate, (SDS) was used to adsorb and dissociate the AuNPs from the formulated AuNPs-SST leaving SST free in solution. Then, the free SST was quantified using HPLC. In brief, 3mL of the purified AuNPs-SST were incubated with 3mg solid SDS at room temperature and left overnight. SDS adsorbed the AuNPs from AuNPs-SST leaving SST free in the supernatant which it can be measured and identified by HPLC.

HPLC analysis was performed for SST using a system with a Degasser (Knauer, Berlin, Germany), LC-10AT pump, FCV-10ATVP gradient mixer, SIL-10ADVP autosampler, CTO-6A column oven, SPD-10AV UV-detector, RF-551 fluorescence detector and SCL-10AVP controller (Shimadzu, Duisburg, Germany). HPLC analysis was performed for SST using linear gradient method from 26% to 39% acetonitrile in water, with 0. 1% TFA, as mobile phase was applied over 15 minutes at a flow rate of

1.0mL/minute. The samples were separated at a temperature of 40°C using a C18-reversed Precolumn (LC 318, 4.6mMx5.0mm). Chromatograms were detected by UV detection at 210nm and 274nm (33).

Identification of the attached SST to AuNPs using sodium dodecyl sulfate polyacrylamide gel electrophoresis

The adsorbed SST to AuNPs was determined using SDS-PAGE as previously reported (34-35). In brief, 21μL of AuNPs-SST was mixed with 7µL modified SDS-PAGE sample buffer. Without heating, the samples were loaded in duplicates onto a 6% SDS-PAGE gel. Then, the normal gel running procedure was followed. Putamol was used to over fill the separating gel. Electrophoresis was run in a constant mode at 100mA using Pharmacia Biotech Electrophoresis Power Supply EPS (Bridge Path Scientific, 4841 International Boulevard, Frederick, MD 21703). It was running on discontinuous buffer system. The running was also using separating gels (6%) and collecting gel (1.2mL acrylimide, 2mL collecting gel buffer, 5µL TEMED and 80µL APS 10%). 10µL of protein ladder of 19, 26, 34, 48, 85, or 117kDa were used as control protein. Gels were stained by Coomassie Brilliant Blue G-25 dispersion.

UV-VIS spectroscopy of AuNPs and AuNP-SST

UV-VIS absorption spectra of the citrate-AuNPs, MUA-AuNPs and AuNPs decorated with SST were recorded using an Uvikon 941UV-VIS absorbance spectrophotometer (Kontron Instruments GmbH). It was taken five spectra of each gold colloid suspension in the range from 400to700nm. The absorbance measurements were made using 0.5cm path length quartz cuvettes. The SPR is clearly visible as a peak in the range between 514 and 550nm.

Cellular uptake study

HCC1806 cells were used to study the cellular uptake of SST-decorated AuNPs. HCC-1806 cells express all types of SSTRs. SSTRs expression was confirmed by Reverse Transcription Polymerase Chain Reaction (RT-PCR) (36). HCC-1806 cells were cultured in T-75 tissue culture flasks in RPMI 1640 supplemented with 10% FCS (37).

Cellular uptake study of AuNPs-SST using inductively coupled plasma-optical emission spectroscopy ICP-OES

To determine quantatively the number of AuNPs entered per cell, HCC-1806 cells were incubated for 1 hour at 37°C with 1mL of 100nM of citrate-AuNPs and AuNPs-SST. The incubation was performed in 1mL of serum-containing culture medium with serum free Leibowitz medium in T-75 tissue culture flasks. To displace the bound AuNPs-SST, the cells were incubated prior to the experiment for 20 minutes with 100µL of 1mM antagonist (cyn-164806). The AuNPs concentrations were determined in 96-well plate using an Uvikon 941UV-VIS absorbance spectrophotometer (Kontron Instruments GmbH) (38). To harvest cells, 2mL of trypsin-EDTA was added to the flask. The flasks were incubated at 37±0.5°C for 3 minutes to allow cell detachment. The cells were washed with DPBS two times, followed by centrifugation at 300×*g* (18±0.5°C) for 5 minutes in order to pellet the cells. The cells were transferred to a 5mL glass vials.

ICP-OES sample preparation and determination of AuNPs

This technique is specifically used to determine the concentration of Au^{3+} metals, minor and major concentrations as a previously reported (30, 39). Typically, 500µL of each sample containing AuNPs was mixed with 200µL of freshly prepared aqua regia

then diluted to 5mL with Millipore water. The Au^{3+} content of the digested cells was determined using ICP-OES on a JY-70 PLUS (Jobin Yvon Instruments S.A.). The plasma flow was 16mL/minute argon. Concentrations of 1, 10 and 100ppm were used as a standard concentration of gold (III) chloride. The numbers of AuNPs per cell were determined by ICP-OES (for details of calculation refer the Supporting Information).

Statistical analysis

Cellular uptake study was subjected to statistical analysis using One-way analysis of variance (ANOVA). Minitab® 16 Statistical Software with the Tukey's multiple comparison was employed for comparing the formulations with each other. Statistically significant differences were assumed when $p<0.05$.

Results and discussion

Preparation and characterization of AuNPs

Citrate coated AuNPs were synthesized as reported previously (30). During this synthesis, a color change was observed when tri-sodium citrate was added to $HAuCl_4$ solution. The solution was initially of yellowish color. After the citrate was added, the color changed first to light blue, dark blue, then purple, dark purple, and finally red to purple in color (Figure 2).

Insert Figure 2 here

The obtained series of colour change indicated the formation of small and uniform citrate-AuNPs via the citrate-reduction method using a molar ratio of 3:1 tri-sodium citrate to $HAuCl_4$. Furthermore, the formulated citrate-AuNPs were uniform in particle size of 19.3±0.5nm and had a negative surface charge of - 43.4±0.5mV (Figure 3).

Size (hydrodynamic diameter), Polydispersity index (PDI) and zeta potential of particles are parameters that indicate the stability of nanoparticles(40-41). High PDI indicates the heterogeneity of the particle size in suspension. While smaller PDI values indicate the homogeneity of the particle size in suspension. It was reported that PDI lower than 0.2 is considered to be ideal hence, the particle size distribution falls within a narrow range of size (40, 42-45). The surface charge also plays an important role in the stability of the nanoparticles and the magnitude of zeta potential is indicative of the colloidal stability of the system (46).

In addition, the mean count rate and PDI were monitored as shown in (Figure 3). The high-count rate 185 kpcs, indicated that the concentration of nanoparticles was high

enough for measurements. Furthermore, the PDI was very small 0.16, indicating that the colloidal AuNPs were uniform and has a very narrow size distribution range.

Insert Figure 3 here

Stabilization of the synthesized AuNPs using 11-MUA

A stronger stabilizing agent, 11-MUA, was used instead of citrate to achieve successful coating of AuNPs with SST. 11-MUA is a thiol compound that binds strongly to gold surfaces. Citrate-AuNPs were coated with 11-MUA at pH 11. The carboxyl group of 11-MUA is deprotonated at pH 11 and can stabilize the particle dispersion via electrostatic repulsion (32). After coating of AuNPs with 11-MUA, the size increased to 23.5±0.05nm with a PDI of about 0.2 (Figure 4). After the purification of MUA-AuNPs, the PDI decreased to a value of 0.1 indicating that the free 11-MUA was removed from the colloidal solution, and MUA-AuNPs turned to a more stable and more monodisperse colloidal solution.

It was found that the zeta potential was highly negative -73.2±0.06mV for crude MUA-AuNPs. After purification, the zeta potential increased to become less negative -65.3±0.1mV, but still high enough to stabilize the particles in an aqueous environment as shown in (Figure 5). On the same time, this highly negative charge is ideal for an adsorptive immobilization of SST.

Insert Figures 4 and 5 here

Influence of different ionic strength on the stability of MUA-AuNPs

Ionic strength is very important for the stability of colloidal nanoparticles (47). In addition, ionic strength is considered one of the most important factors that influence

the adhesion of a molecule to nanoparticles surfaces (30). To determine the ideal ionic strength, different concentrations of NaCl (10, 20 and 30mM) were tried for to choose the probable conc. which stabilize the coating of MUA-AuNPs with SST. Furthermore, the stability of the particles at different ionic strengths was determined by monitoring the change in the particles size, zeta potential and PDI. A concentration of 10mM NaCl proved to be a suitable ionic strength for maintaining a small hydrodynamic diameter and low PDI of MUA-AuNPs during the coating and purification processes. On the other hand, MUA-AuNPs with 20mM and 30mM NaCl, showed aggregation with undefined particle sizes. The PDI of MUA-AuNPs of 10mM NaCl was 0.2±0.04. In contrast, the PDI for 20 and 30mM NaCl was 0.34±0.8 and 0.5±0.3; respectively as shown in (Figure 6) which indicated the beginning of particle aggregation and instability. This could be attributed to the increase in PDI in these higher molar concentrations. It was found that increasing the ionic strength led to a decrease in the Debye length between the particles concomitant with particles aggregation (48).

Zeta potential analysis was performed for identification of the change in the surface charge of MUA-AuNPs at different ionic strengths (Figure 7). The MUA-AuNPs mixed with 100µL of 10mM NaCl had a high negative surface charge of -60.7±2.1 owing to the presence of carboxylate anions from 11-MUA. Increasing the ionic strength to 20and 30mM decreased the negative surface potential to a value of -20.6±0.5 and -19.7±6.8mV; respectively, leading to the aggregation of the nanoparticles as shown in (Figure 7). This was accompanied by a color change from red to blue as depicted in (Figure 2). This interaction is most likely due to increased

Van der Waals forces (46, 49-51). From the above results, it was clear that AuNPs are reasonably stable after 11-MUA coating and resist aggregation in the presence of up to 10mM NaCl.

Insert Figures 6 and 7 here.

Coating of MUA-AuNPs with SST

The coating process of SST on MUA-AUNPs could be performed according to the adsorption between oppositely charged groups. SST, which has a positive charge, was adsorbed on a negatively charged MUA-AuNPs. Different concentrations of SST were tried to choose the best and high-adsorbed amounts of SST. The amount of SST adsorbed to AuNPs seemed to increase from 20nM to 200nM. The particle sizes increased to 21.7±0.06, 22.4±0.3, 23.5±0.2, 25.05±0.07 and 28.3±0.4 for different SST concentrations of 20, 40, 60, 100 and 200nM; respectively with acceptable PDI as shown in (Table 1). After purification, the nanoparticles were stable without aggregation. However, particles coated with a concentration of 200nM SST showed aggregates after six hours, indicating that they are not acceptable preparations for a long-term stability. For that reason, the ideal SST concentration to be used for coating was chosen to be 100nM because the formed particles were stable in size and did not form aggregates.

(Insert Table 1 here)

Therefore, zeta potential was measured to confirm the successful coating of AuNPs with SST. Citrate-AuNPs had a zeta potential of -40.9±4.9mV. After deposition of 11-MUA, it became more negative -60.8±2.65mV, indicating that citrate was replaced

with 11-MUA and the surface of gold coated carboxylic acid groups. Moreover, the zeta potential of all the investigated particles was initially negative then, after coating with different concentrations of 20-200nM SST, it became more and more positive. Furthermore, AuNPs-SST at 60, 100 and 200nM showed a reversal of the zeta potential values from negative to positive (16.9, 20.3 and 29.3mV; respectively, Table 1). Thus, zeta potential study proved the successful loading of SST on the surface of MUA-AuNPs.

The significance of 11-MUA for coating of SST-AuNPs

Since the citrate-AuNPs have a negative surface charge and SST has a positive charge. SST might be deposited on the surface of AuNPs without of 11-MUA as an intermediate coating. To investigate this aspect, AuNPs were mixed with SST solution directly. The results of this experiment showed that 11-MUA is essential for coating of SST to AuNPs. Since, the absence of 11-MUA during the coating of citrate-AuNPs with SST led to an aggregation of AuNPs. Accordingly, the deposition of SST on MUA-AuNPs showed no aggregation even at higher concentration of SST about 100nM (Figure 8a). While citrate-AuNPs formed aggregates after all purification steps even it was coated with 20nM of SST (Figure 8b).

Insert Figure 8 a&b here

Hence, it was worthy to use 11-MUA for coating of SST to AuNPs, since it make the AuNPs more stable and can adsorb easily SST. Furthermore, the aggregation observed in citrate-AuNPs could be possibly attributed to the failure of SST to replace the citrate anion on the surface of AuNPs which may formed as positive negative complex or

could be the disulfide bond of SST was reduced by citrate that make the particles aggregated.

Dissociation of AuNPs-SST by sodium dodecyl sulphate (SDS)

The effects of ionic surfactants like SDS on AuNPs-SST were studied using HPLC. At pH 7.0, anionic surfactants such as SDS induce peptide dissociation for AuNPs-SST. For this reason, SDS was used to confirm the adsorption of SST to AuNPs. Figure 9 shows the chromatograms of SST and SST dissociated from AuNPs-SST. The dissociation of SST from AuNPs showed a single peak eluted at about 3.6 minutes. The chromatogram showed no degradation products. The SST dissociated from AuNPs was eluted earlier than the free SST, because it was less hydrophilic due to the presence of some traces of 11-MUA. Thus, confirmed the adsorption of SST to AuNPs, which then dissociated from the AuNPs with SDS.

Insert Figure 9 here

SST adsorbed to the surface of AuNPs was also analyzed using SDS-PAGE. Figure 10 shows the SDS-PAGE containing a single band for AuNPs-SST (lane 5) that does not move. This confirmed the attachment of SST to the AuNPs which hinder the peptide from moving in the applied electric field(52-53). On the other hand, the 100nM concentration of SST and citrate-AuNPs showed no bands (lane 3 and lane 4; respectively). However, increasing the concentration of SST to 100nM resulted in appearance of band (lane 2) which is also confirmed the attachment of SST to AuNPs.

Insert Figure 10 here

UV-VIS spectroscopy of AuNPs and AuNPs decorated with SST

The optical properties of AuNPs are highly dependent on the nanoparticle diameter. Smaller nanoparticles absorb light and have peaks near 520nm, while larger spheres exhibit increased scattering and have peaks shifted towards longer wavelengths (known as red-shif). Furthermore, larger spheres scatter more light because they have larger optical cross sections, and their albedo (a ratio of scattering to total extinction) increases with size. AuNPs are often used as bio-imaging tags in dark field microscopy techniques, where the scattering from individual nanoparticles with diameters larger than 40-50nm can be observed(54). The UV-VIS spectra of citrate-AuNPs, MUA-AuNPs and AuNPs-SST showed a small red shift in the surface Plasmon resonance peak. The shifts observed were of values of 5 and 4nm for MUA-AuNPs and AuNPs-SST; respectively as shown in (Figure 11). This could be possibly attributed to the deposition of 11-MUA and SST on AuNPs and increasing the nanoparticles size.

Insert Figure 11 here

Cellular uptake study

To study the cellular uptake of AuNPs-SST, HCC-1806 cells were chosen as a model cell lines. HCC-1806 cells were incubated with citrate-AuNPs (as control nanoparticles) and AuNPs-SST for 1 hour in RPMI 1640 medium containing serum. HCC-1806 cells took up all types of AuNPs and the average amount of AuNPs per cell strongly depended on the type of the top layer. Since all kinds of AuNPs are of nearly similar sizes but possess different outer layers, this suggests that surface properties may strongly affect interactions with the cells. The number of AuNPs per cell was determined by ICP-OES. The initial concentration of AuNPs in the culture medium

was 100nM for citrate-AuNPs, MUA-AuNPs and AuNPs-SST. AuNPs-SST were internalized in significantly ($p<0.05$; ANOVA/Tukey) higher amounts (estimated number, 15393±656per cell) more than citrate-AuNPs and AuNPs-SST (estimated number 3779±758 and 8649±570per cell; respectively) in the presence of the antagonist (cyn 154806) as shown in (Figure 12). However, the higher amounts of antagonist up to 1mM displaced the nanoparticles from the receptor. Hence, it can be concluded that the difference in the cellular uptake of AuNPs-SST is due to differences in surface properties and not in the size of AuNPs. Nanoparticle interaction with cells is an issue of importance for targeting of these particles to different cells. These results On the one hand there counteract the evidence of unwanted interactions such that particles enter cells with a non-specific way when they are exposed to colloids. SST as SSTRs agonist could easily fit on the SSTRs which increase the internalization of AuNPs, whilest blocking of these receptors by antagonist like cyn-154806 led to internalization of AuNPs.

Insert Figure 12 here

Conclusions

Citrate-AuNPs were efficiently synthesized via the citrate-reduction method. They are uniform in size 19.3±0.5nm and had a negative charge of -43.4±0.5mV. Moreover, AuNPs were stable, resist the aggregation and successfully coated with SST after binding with 11-MUA instead of citrate ions. All analytical tools used in our study e.g., DLS, SDS-PAGE and UV-VIS absorption spectra confirmed the attachment of SST to AuNPs. In addition, significantly ($p<0.05$; ANOVA/Tukey) higher amounts AuNPs-SST particles internalized per cell in HCC-1806 cell lines compared to citrate-AuNPs and AuNPs-SST in the presence of antagonists. Such internalization depends on the surface properties of the cells not on the size of particles as shown when the receptors were blocked by incorporation of antagonist. Finally, the proof of principle has been addressed and we will focusing our research in the future in the delivery of these novel AuNPs coated with SST to various tumor cells.

Acknowledgment

The authors would like to thank also the Department of Pharmaceutics and Industrial Pharmacy, Al-Azhar University and the Department of Industrial Pharmacy, Assiut University, Assiut, Egypt for their financial support.

Declaration of interest

The authors report no declarations of interest.

References

1. Huang KJ, Li J, Liu YM, Cao XY, Yu S, Yu M. Disposable immunoassay for hepatitis B surface antigen based on a graphene paste electrode functionalized with gold nanoparticles and a Nafion-cysteine conjugate. Microchimica Acta. 2012 Jun;177(3-4):419-26.

2. Saleh M, Soliman H, Haenen O, El-Matbouli M. Antibody-coated gold nanoparticles immunoassay for direct detection of Aeromonas salmonicida in fish tissues. Journal of Fish Diseases. 2011 Nov;34(11):845-52.

3. Bhattacharyya S, Khan JA, Curran GL, Robertson JD, Bhattacharya R, Mukherjee P. Efficient Delivery of Gold Nanoparticles by Dual Receptor Targeting. Advanced Materials. 2011 Nov 16;23(43):5034-8.

4. Kang B, Mackey MA, El-Sayed MA. Nuclear targeting of gold nanoparticles in cancer cells induces DNA damage, causing cytokinesis arrest and apoptosis. J Am Chem Soc. 2010 Feb 10;132(5):1517-9.

5. Hoyer D, Bell GI, Berelowitz M, Epelbaum J, Feniuk W, Humphrey PP, et al. Classification and nomenclature of somatostatin receptors. Trends Pharmacol Sci. 1995 Mar;16(3):86-8.

6. Patel YC. Somatostatin and its receptor family. Front Neuroendocrinol. 1999 Jul;20(3):157-98.

7. Rufini V, Calcagni ML, Baum RP. Imaging of neuroendocrine tumors. Semin Nucl Med. 2006 Jul;36(3):228-47.

8. Taniyama Y, Suzuki T, Mikami Y, Moriya T, Satomi S, Sasano H. Systemic distribution of somatostatin receptor subtypes in human: an immunohistochemical study. Endocr J. 2005 Oct;52(5):605-11.

9. Long JB. Spinal subarachnoid injection of somatostatin causes neurological deficits and neuronal injury in rats. Eur J Pharmacol. 1988 May 10;149(3):287-96.

10. Reubi JC, Waser B, Schaer JC, Laissue JA. Somatostatin receptor sst1-sst5 expression in normal and neoplastic human tissues using receptor autoradiography with subtype-selective ligands. Eur J Nucl Med. 2001 Jul;28(7):836-46.

11. Rivera JA, Alturaihi H, Kumar U. Differential regulation of somatostatin receptors 1 and 2 mRNA and protein expression by tamoxifen and estradiol in breast cancer cells. J Carcinog. 2005 Jul 14;4(1):10.

12. Virgolini I, Traub T, Novotny C, Leimer M, Fuger B, Li SR, et al. Experience with indium-111 and yttrium-90-labeled somatostatin analogs. Curr Pharm Des. 2002;8(20):1781-807.

13. Weiner RE, Thakur ML. Radiolabeled peptides in oncology: role in diagnosis and treatment. BioDrugs. 2005;19(3):145-63.

14. Sharma K, Srikant CB. Induction of wild-type p53, Bax, and acidic endonuclease during somatostatin-signaled apoptosis in MCF-7 human breast cancer cells. Int J Cancer. 1998 Apr 13;76(2):259-66.

15. Zhang D, Lee HF, Pettit SC, Zaro JL, Huang N, Shen WC. Characterization of transferrin receptor-mediated endocytosis and cellular iron delivery of recombinant human serum transferrin from rice (Oryza sativa L.). BMC Biotechnol. 2012 Nov 30;12(1):92.

16. Thomsen LB, Lichota J, Larsen TE, Linemann T, Mortensen JH, du Jardin KG, et al. Brain Delivery Systems via Mechanism Independent of Receptor-Mediated Endocytosisi and Adsorptive Mediated Endocytosis. Curr Pharm Biotechnol. 2012 Sep 19.

17. Wang H, Wu L, Reinhard BM. Scavenger receptor mediated endocytosis of silver nanoparticles into J774A.1 macrophages is heterogeneous. ACS Nano. 2012 Aug 28;6(8):7122-32.

18. Delehanty JB, Mattoussi H, Medintz IL. Delivering quantum dots into cells: strategies, progress and remaining issues. Anal Bioanal Chem. 2009 Feb;393(4):1091-105.

19. Chen B, Liu QL, Zhang YL, Xu L, Fang XH. Transmembrane Delivery of the Cell-Penetrating Peptide Conjugated Semiconductor Quantum Dots. Langmuir. 2008 Oct 21;24(20):11866-71.

20. Kelf TA, Sreenivasan VKA, Sun J, Kim EJ, Goldys EM, Zvyagin AV. Non-specific cellular uptake of surface-functionalized quantum dots. Nanotechnology. 2010 Jul 16;21(28).

21. Moaeen-Ud-Din M, Yang LG. Evolutionary history of the somatostatin and somatostatin receptors. J Genet. 2009 Apr;88(1):41-53.

22. Reisine T, Woulfe D, Raynor K, Kong H, Heerding J, Hines J, et al. Interaction of somatostatin receptors with G proteins and cellular effector systems. Ciba Found Symp. 1995;190:160-7; discussion 7-70.

23. Bell GI, Yasuda K, Kong H, Law SF, Raynor K, Reisine T. Molecular biology of somatostatin receptors. Ciba Found Symp. 1995;190:65-79; discussion 80-8.

24. Florio T, Rim C, Hershberger RE, Loda M, Stork PJS. The Somatostatin Receptor Sstr1 Is Coupled to Phosphotyrosine Phosphatase-Activity in Cho-K1 Cells. Molecular Endocrinology. 1994 Oct;8(10):1289-97.

25. Lahlou H, Guillermet J, Hortala M, Vernejoul F, Pyronnet S, Bousquet C, et al. Molecular signaling of somatostatin receptors. Ann N Y Acad Sci. 2004 Apr;1014:121-31.

26. Kimling J, Maier M, Okenve B, Kotaidis V, Ballot H, Plech A. Turkevich method for gold nanoparticle synthesis revisited. J Phys Chem B. 2006 Aug 17;110(32):15700-7.

27. Frens G. Controlled Nucleation for Regulation of Particle-Size in Monodisperse Gold Suspensions. Nature-Phys Sci. 1973;241(105):20-2.

28. Abdellatif AAH, editor. Gold Nanoparticles Decorated With Octreotide For Somatostatin Receptors Targeting: J. of pharmaceutical science & research; 2015.

29. Bhattacharjee RR, Mandal TK. Polymer-mediated chain-like self-assembly of functionalized gold nanoparticles. J Colloid Interf Sci. 2007 Mar 1;307(1):288-95.

30. Elbakry A, Zaky A, Liebkl R, Rachel R, Goepferich A, Breunig M. Layer-by-Layer Assembled Gold Nanoparticles for siRNA Delivery. Nano Lett. 2009 May;9(5):2059-64.

31. Chang CW, Chu SP, Tseng WL. Selective extraction of melamine using 11-mercaptoundecanoic acid-capped gold nanoparticles followed by capillary electrophoresis. Journal of Chromatography A. 2010 Dec 3;1217(49):7800-6.

32. Lin SY, Tsai YT, Chen CC, Lin CM, Chen CH. Two-step functionalization of neutral and positively charged thiols onto citrate-stabilized Au nanoparticles. Journal of Physical Chemistry B. 2004 Feb 19;108(7):2134-9.

33. Brizzi V, Corradini D. Rapid Analysis of Somatostatin in Pharmaceutical Preparations by Hplc with a Micropellicular Reversed-Phase Column. J Pharmaceut Biomed. 1994 Jun;12(6):821-4.

34. Khalkhali-Ellis Z. An improved SDS-polyacrylamide gel electrophoresis for resolution of peptides in the range of 3.5-200kDa. Prep Biochem. 1995 Feb-May;25(1-2):1-9.

35. Brandl F, Hammer N, Blunk T, Tessmar J, Goepferich A. Biodegradable hydrogels for time-controlled release of tethered peptides or proteins. Biomacromolecules. 2010 Feb 8;11(2):496-504.

36. Seitz S, Schally AV, Gluck S, Rick F, Szalontay L, Hohla F, et al. Effective treatment of triple-negative breast cancer with targeted cytotoxic somatostatin analogue AN-162 (AEZS-124). J Clin Oncol. 2009 May 20;27(15):-.

37. Keller PJ, Lin A, Arendt LM, Klebba I, Jones AD, Rudnick JA, et al. Mapping the cellular and molecular heterogeneity of normal and malignant breast tissues and cultured cell lines. Breast Cancer Res. 2010 Oct 21;12(5):R87.

38. Haiss W, Thanh NT, Aveyard J, Fernig DG. Determination of size and concentration of gold nanoparticles from UV-vis spectra. Anal Chem. 2007 Jun 1;79(11):4215-21.

39. Chithrani BD, Ghazani AA, Chan WCW. Determining the size and shape dependence of gold nanoparticle uptake into mammalian cells. Nano Lett. 2006 Apr;6(4):662-8.

40. Pereira-Lachataignerais J, Pons R, Panizza P, Courbin L, Rouch J, Lopez O. Study and formation of vesicle systems with low polydispersity index by ultrasound method. Chem Phys Lipids. 2006 Apr;140(1-2):88-97.

41. Moraes CM, De Paula E, Rosa AH, Fraceto LF. Physicochemical Stability of Poly(lactide-co-glycolide) Nanocapsules Containing the Local Anesthetic Bupivacaine. Journal of the Brazilian Chemical Society. 2010;21(6):995-1000.

42. Aghajani M, Shahverdi AR, Amani A. The Use of Artificial Neural Networks for Optimizing Polydispersity Index (PDI) in Nanoprecipitation Process of Acetaminophen in Microfluidic Devices. AAPS PharmSciTech. 2012 Sep 21.

43. Lewis G, Li Y. Dependence of in vitro fatigue properties of PMMA bone cement on the polydispersity index of its powder. J Mech Behav Biomed Mater. 2010 Jan;3(1):94-101.

44. Rosenfeld C, Serra C, Brochon C, Hadziioannou G. Influence of micromixer characteristics on polydispersity index of block copolymers synthesized in continuous flow microreactors. Lab Chip. 2008 Oct;8(10):1682-7.

45. Vieville J, Tanty M, Delsuc MA. Polydispersity index of polymers revealed by DOSY NMR. J Magn Reson. 2011 Sep;212(1):169-73.

46. Kaufman ED, Belyea J, Johnson MC, Nicholson ZM, Ricks JL, Shah PK, et al. Probing protein adsorption onto mercaptoundecanoic acid stabilized gold nanoparticles and surfaces by quartz crystal microbalance and zeta-potential measurements. Langmuir. 2007 May 22;23(11):6053-62.

47. Santander-Ortega MJ, Jodar-Reyes AB, Csaba N, Bastos-Gonzalez D, Ortega-Vinuesa JL. Colloidal stability of pluronic F68-coated PLGA nanoparticles: a variety of stabilisation mechanisms. J Colloid Interface Sci. 2006 Oct 15;302(2):522-9.

48. Parab HJ, Huang JH, Lai TC, Jan YH, Liu RS, Wang JL, et al. Biocompatible transferrin-conjugated sodium hexametaphosphate-stabilized gold nanoparticles: synthesis, characterization, cytotoxicity and cellular uptake. Nanotechnology. 2011 Sep 30;22(39):395706.

49. Wang G, Sun W. Optical limiting of gold nanoparticle aggregates induced by electrolytes. J Phys Chem B. 2006 Oct 26;110(42):20901-5.

50. Aryal S, Remant BK, Narayan B, Kim CK, Kim HY. Study of electrolyte induced aggregation of gold nanoparticles capped by amino acids. J Colloid Interface Sci. 2006 Jul 1;299(1):191-7.

51. Aili D, Enander K, Rydberg J, Lundstrom I, Baltzer L, Liedberg B. Aggregation-induced folding of a de novo designed polypeptide immobilized on gold nanoparticles. J Am Chem Soc. 2006 Feb 22;128(7):2194-5.

52. Lee SH, Zhang ZP, Feng SS. Nanoparticles of poly(lactide) - Tocopheryl polyethylene glycol succinate (PLA-TPGS) copolymers for protein drug delivery. Biomaterials. 2007 Apr;28(11):2041-50.

53. Nishio K, Gokon N, Hasegawa M, Ogura Y, Ikeda M, Narimatsu H, et al. Identification of a chemical substructure that is immobilized to ferrite nanoparticles (FP). Colloids and Surfaces B-Biointerfaces. 2007 Feb 15;54(2):249-53.

54. Elbakry A, Zaky A, Liebl R, Rachel R, Goepferich A, Breunig M. Layer-by-layer assembled gold nanoparticles for siRNA delivery. Nano Lett. 2009 May;9(5):2059-64.

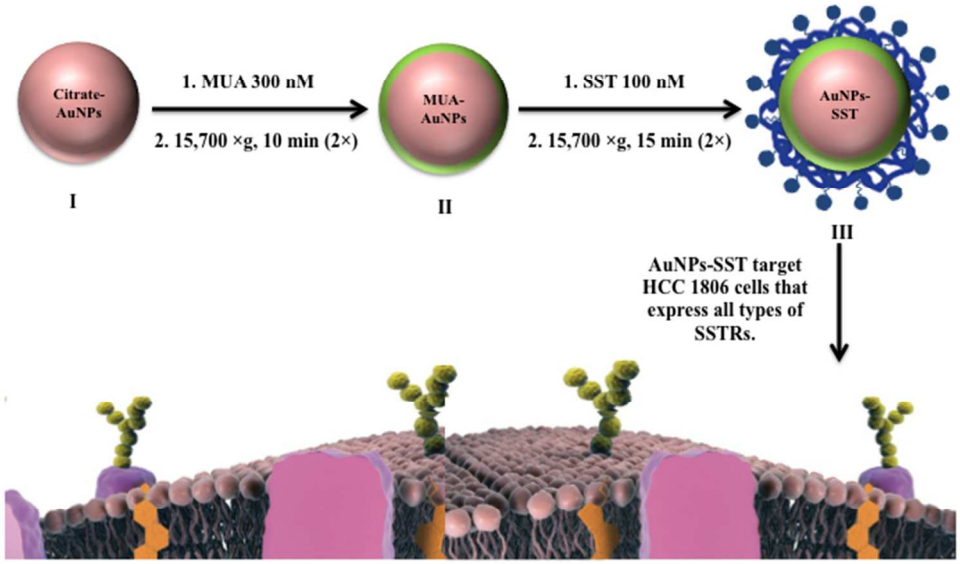

Figure 1: Schematic diagram for deposition of SST onto MUA-AuNPs. 10mM of NaCl used as isotonic solution. MUA-AuNPs was added drop-wise to 10µL of concentration of 100nM SST stirred for 30 minutes and purified by centrifugation at 15,700×g for 15 minutes.
254x190mm (72 x 72 DPI)

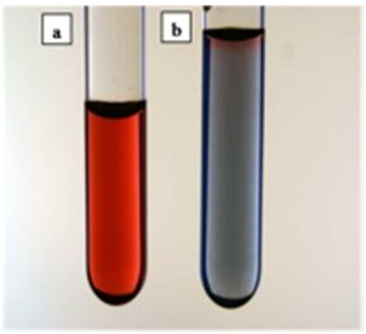

Figure 2: Image of a) monodispersed AuNPs with red to purple color, b) polydispersed aggregated AuNPs with a blue color.
63x57mm (72 x 72 DPI)

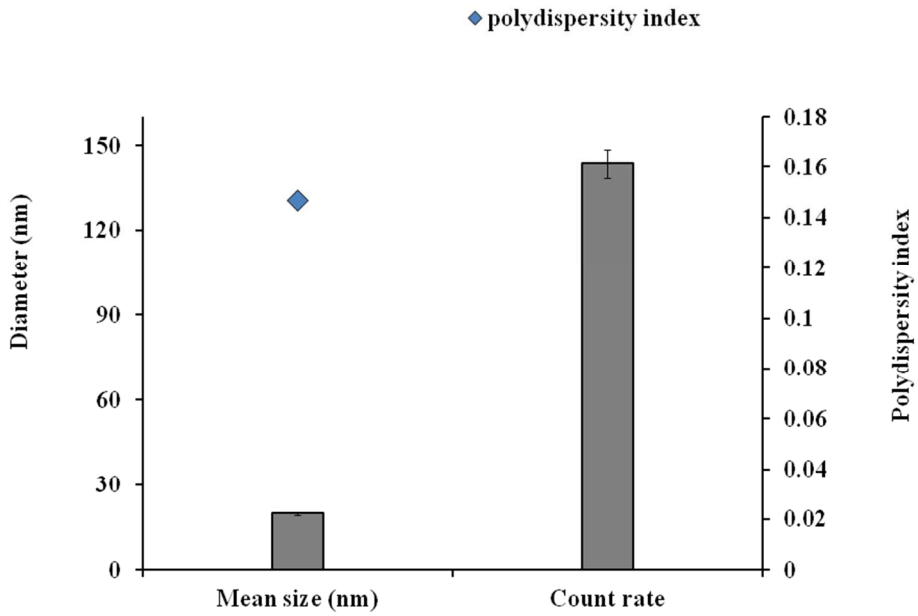

Figure 3: Particle size distribution, count rate as well as the polydispersity index (black diamond) of citrate-AuNPs of 19nm using DLS.
254x190mm (96 x 96 DPI)

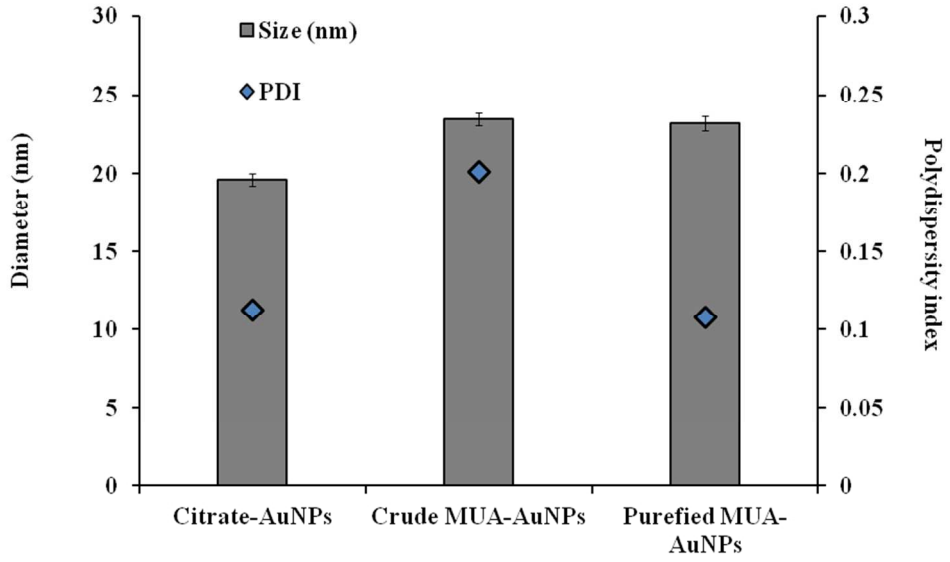

Figure 4: The hydrodynamic diameter as well as PDI of citrate-AuNPs, crude MUA-AuNPs and purified MUA-AuNPs.
254x190mm (96 x 96 DPI)

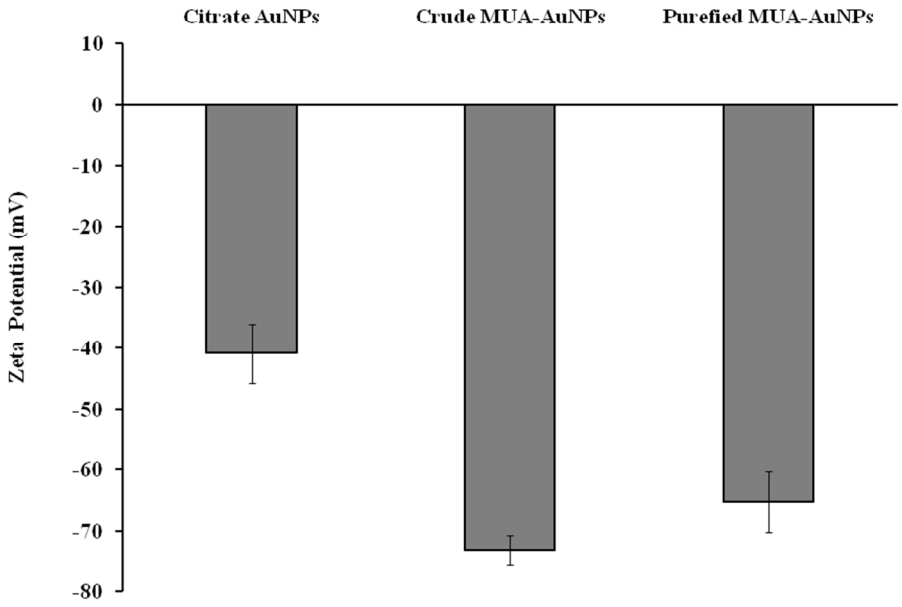

Figure 5: Zeta potential of citrate-AuNPs, crude MUA-AuNPs and purified MUA-AuNPs as a function of stability.
254x190mm (96 x 96 DPI)

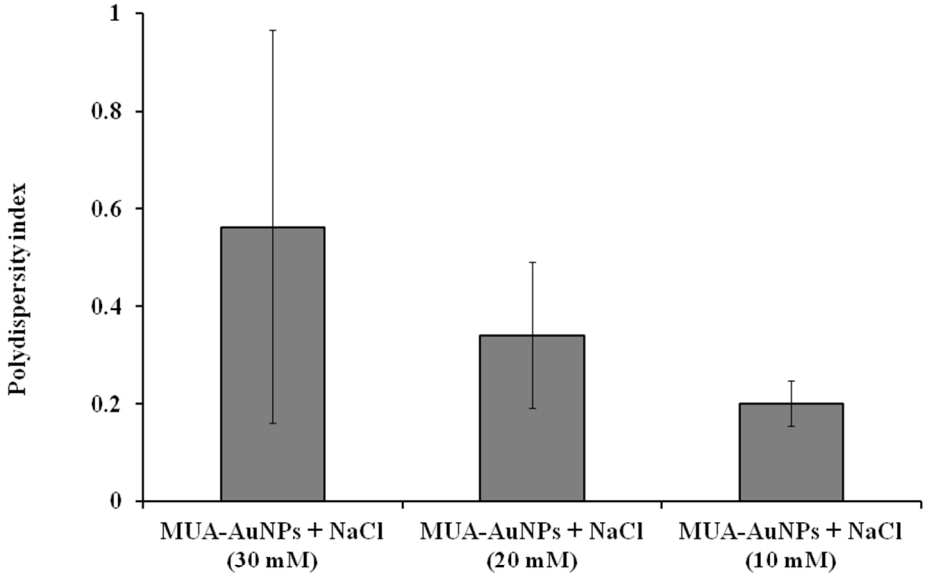

Figure 6: Influence of ionic strength on the polydispersity index of 11-MUA coated AuNPs. The PDI of MUA-AuNPs with 10 mM NaCl is satisfactory low. In contrast, the PDI with 20 and 30 mM NaCl were much higher, which indicate the beginning of aggregation.
254x190mm (96 x 96 DPI)

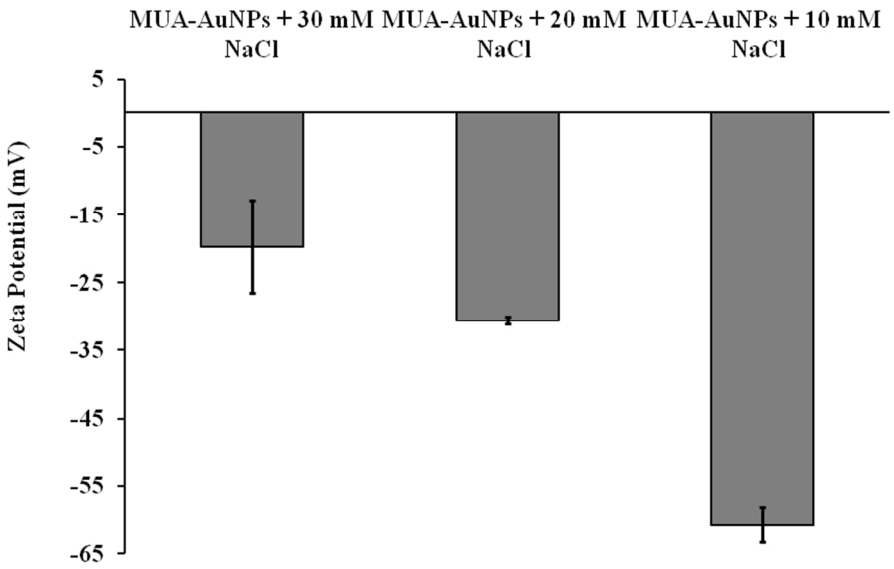

Figure 7: Zeta potential measurements of MUA-AuNPs at different ionic strength (10, 20 and 30)mM NaCl . The MUA-AuNPs mixed with 10mM NaCl had a high negative surface charge. Increasing the ionic strength to 20 and 30mM, decreased the negative surface potential, leading to aggregation of the nanoparticles. This was accompanied by a color change from red to blue.
254x190mm (96 x 96 DPI)

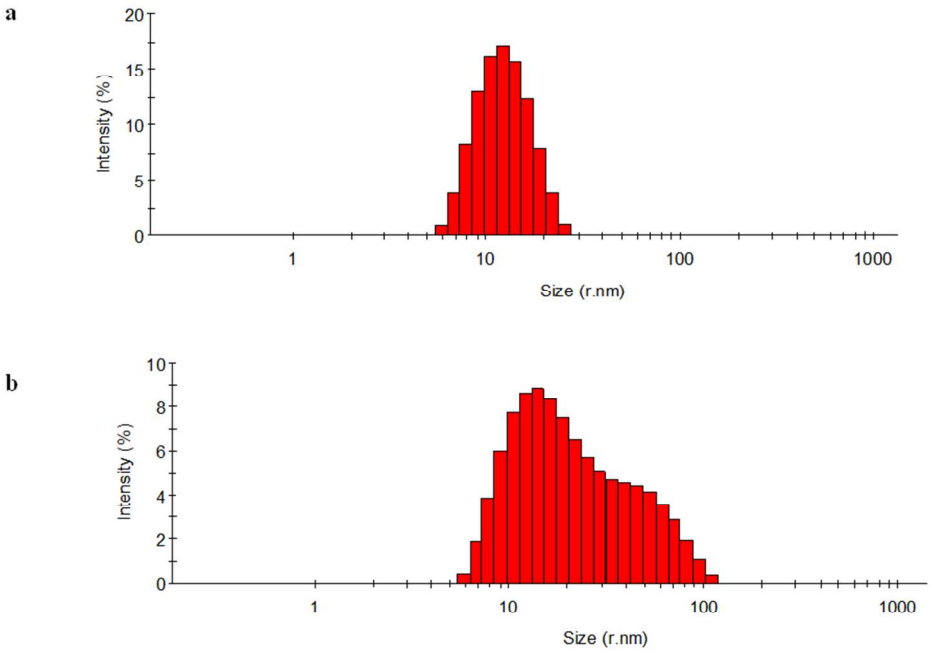

Figure 8: Particle size distribution of AuNPs measured using DLS. a). Coated with SST at concentration of 100nM after deposition on MUA-AuNPs using 10mM NaCl as polyelectrolyte. b). Coated directly with SST at concentration of 20nM after deposition directly on citrate-AuNPs without using 10mM NaCl as polyelectrolyte.
254x190mm (96 x 96 DPI)

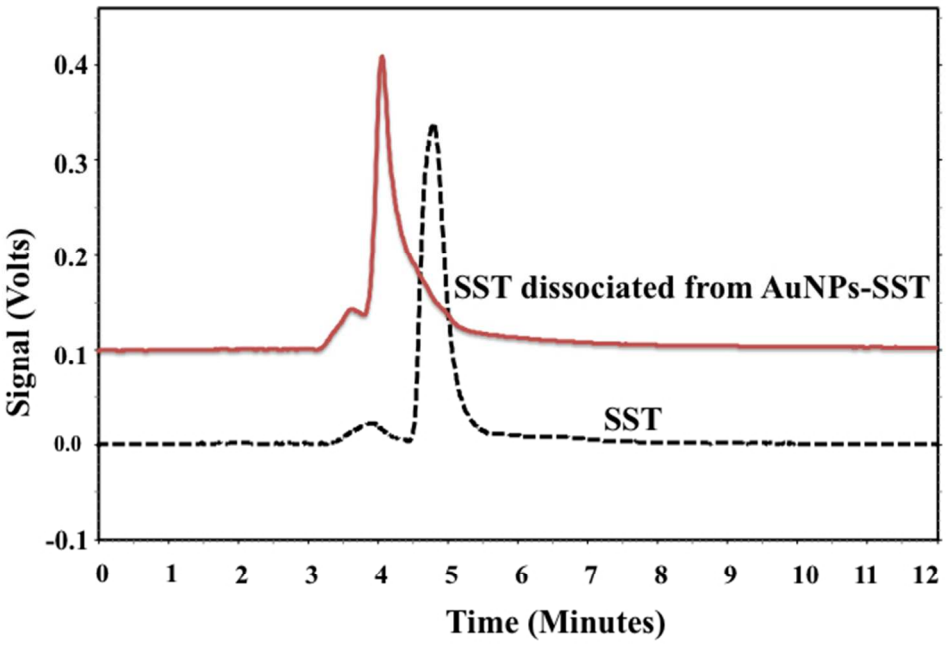

Figure 9: HPLC chromatograms of SST dissociated from AuNPs-SST using SDS.
254x190mm (72 x 72 DPI)

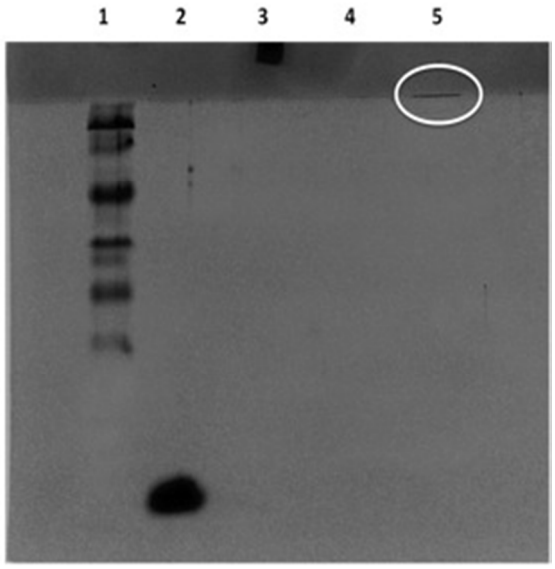

Figure 10: SDS-PAGE analysis for identification of the attachment of SST to AuNPs using 20% acrylamide, and protein ladder 19KDa. For identification of SST, a protein ladder was used (lane 1). High conc. of SST (10mM) (lane 2), 100nM SST (lane 3), citrate-AuNPs (lane 4) and 200nM AuNPs decorated with SST (lane 5).
97x101mm (72 x 72 DPI)

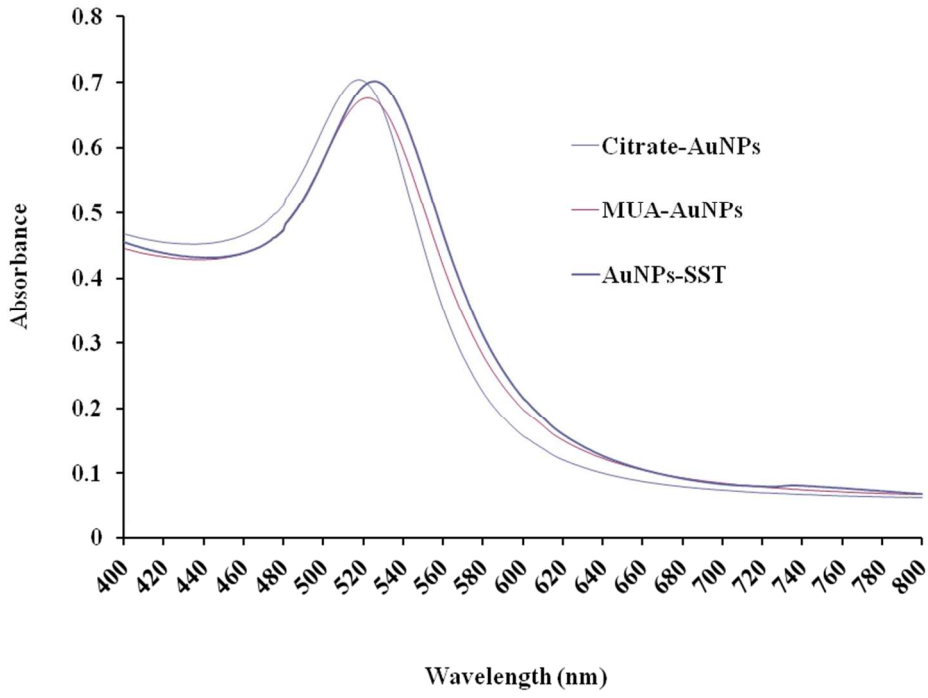

Figure 11: UV-VIS spectra of AuNPs, from top to bottom: citrate-AuNPs, purified AuNPs capped 11-MUA, and purified AuNPs decorated with SST.
254x190mm (96 x 96 DPI)

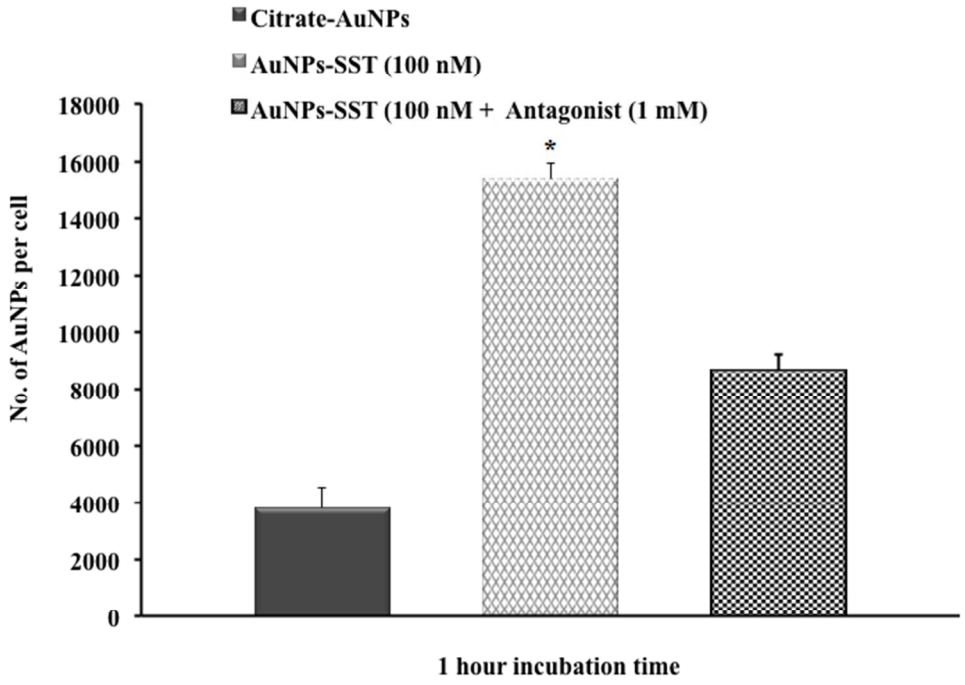

Figure 12: The cellular uptake of AuNPs as determined by ICP-OES and cell counting after 1 hour of incubation. The concentration of AuNPs in the culture medium was 100nM for citrate-AuNPs, and AuNPs-SST. * Significantly different ($p<0.05$; ANOVA/Tukey) verses citrate-AuNPs and AuNPS-SST (100nM + antagonist (1ml).
190x142mm (96 x 96 DPI)

Table 1: Particle size by intensity (percentage), polydispersity index as well as zeta potential of AuNPs coated with different concentrations of SST.

Parameters	SST concentration (nM)	Size (nm)	PDI	zeta potential (mV)
Citrate-AuNPs	0	18.2±0.2	0.14	- 40.93±4.8
MUA-AuNPs	0	20.2±0.1	0.12	- 60.63±2.6
AuNPs-SST	20	21.7±0.1	0.2	- 46.8±2.6
AuNPs-SST	40	22.5±0.3	0.1	- 22.7±1.9
AuNPs-SST	60	23.5±0.2	0.2	16.9±2.9
AuNPs-SST	100	25.1±0.1	0.1	20.3±1.3
AuNPs-SST	200	28.3±0.4	0.2	29.3±1.3

Uptake: unmodified AuNPs per cell

Date	3/10/2013	**Batch**	PCS: 20.83 nm

Concentration in solution/ in cells

d [nm]		18
r [nm]		9
Au^{3+} [ppm]	value cells [1 ppm = 1 mg/kg = 1 mg/l]	0.983333333
Au^{3+} [g/l]	* 10^{-3}	9.83E-04
Au^{3+} [mol/l]	Au^{3+} [g/l] / 197 g/mol [c=m/(M*V)]	4.99E-06
Number Au^{3+} [1/l]	Au^{3+} [mol/l] * L	3.01E+18
Dilution ICP measurement	1	1
Au^{3+} [mol/l]	* Dilution	4.99E-06
Number Au^{3+} [1/l]		3.01E+18
V_{AuNP} [cm^3]	4/3 * π * r^3 * $(10^{-7})^3$ (1nm = 10^{-7}cm)	3.05E-18
m_{AuNP} [g]	19.3 g/cm^3 * V_{AuNP} [cm^3]	5.89E-17
Mol atoms per AuNP [mol]	m_{AuNP} / 197g/mol	2.99E-19
Atoms per AuNP	Atoms per AuNP [mol] * L	1.80E+05
Number AuNP per l [1/l]	Au^{3+} [1/l] * Atoms per AuNP	1.67E+13
AuNP [mol/l]	Number AuNP per l / L	2.77E-11
Number AuNP per µl [1/µl]	Number AuNP / l / 1000000	1.67E+07
Number AuNP 5 ml volumetric flask		8.34E+10

Concentration in cells

Number AuNP / 5 ml flask	8.34E+10
Number of cells total	21938000
Number AuNP / cell	3.80E+03

Uptake: AuNPs-SST per cell

Date	3/10/2013	**Batch**	PCS: 26.84 nm

Concentration in solution/ in cells

d [nm]			25.1
r [nm]			12.55
Au^{3+} [ppm]	value cells	[1 ppm = 1 mg/kg = 1 mg/l]	10.7
Au^{3+} [g/l]	* 10^{-3}		1.07E-02
Au^{3+} [mol/l]	Au^{3+} [g/l] / 197 g/mol [c=m/(M*V)]		5.43E-05
Number Au^{3+} [1/l]	Au^{3+} [mol/l] * L		3.27E+19
Dilution ICP measurement	1		1
Au^{3+} [mol/l]	* Dilution		5.43E-05
Number Au^{3+} [1/l]			3.27E+19
V_{AuNP} [cm^3]	$4/3 * \pi * r^3 * (10^{-7})^3$ (1nm = 10^{-7}cm)		8.28E-18
m_{AuNP} [g]	19.3 g/cm^3 * V_{AuNP} [cm^3]		1.60E-16
Mol atoms per AuNP [mol]	m_{AuNP} / 197g/mol		8.11E-19
Atoms per AuNP	Atoms per AuNP [mol] * L		4.88E+05
Number AuNP per l [1/l]	Au^{3+} [1/l] * Atoms per AuNP		6.70E+13
AuNP [mol/l]	Number AuNP per l / L		1.11E-10
Number AuNP per µl [1/µl]	Number AuNP / l / 1000000		6.70E+07
Number AuNP 5 ml volumetric flask			3.35E+11

Concentration in cells

Number AuNP / 5 ml flask	3.35E+11
Number of cells total	21938000
Number AuNP / cell	1.53E+04

	Conc of Au3+ [ppm]
	13
	11
	9.01
	9.45
	10.78
	11
sum	64.24
average	10.706667

Uptake: AuNPs-SST& Antagonist per cell

Date	3/10/2013	**Batch**	PCS: 26.84 nm

Concentration in solution/ in cells

d [nm]		26.84
r [nm]		13.42
Au^{3+} [ppm]	value cells [1 ppm = 1 mg/kg = 1 mg/l]	7.416666667
Au^{3+} [g/l]	* 10^{-3}	7.42E-03
Au^{3+} [mol/l]	Au^{3+} [g/l] / 197 g/mol [c=m/(M*V)]	3.76E-05
Number Au^{3+} [1/l]	Au^{3+} [mol/l] * L	2.27E+19
Dilution ICP measurement	1	1
Au^{3+} [mol/l]	* Dilution	3.76E-05
Number Au^{3+} [1/l]		2.27E+19
V_{AuNP} [cm^3]	4/3 * π * r^3 * $(10^{-7})^3$ (1nm = 10^{-7}cm)	1.01E-17
m_{AuNP} [g]	19.3 g/cm^3 * V_{AuNP} [cm^3]	1.95E-16
Mol atoms per AuNP [mol]	m_{AuNP} / 197g/mol	9.92E-19
Atoms per AuNP	Atoms per AuNP [mol] * L	5.97E+05
Number AuNP per l [1/l]	Au^{3+} [1/l] * Atoms per AuNP	3.80E+13
AuNP [mol/l]	Number AuNP per l / L	6.30E-11
Number AuNP per µl [1/µl]	Number AuNP / l / 1000000	3.80E+07
Number AuNP 5 ml volumetric flask		1.90E+11

Concentration in cells

Number AuNP / 5 ml flask	1.90E+11
Number of cells total	21938000
Number AuNP / cell	8.65E+03

	Conc of Au3+ [ppm]
	6.9
	7.3
	8.2
	7.2
	7.3
	7.6
sum	44.5
average	7.4166667